International Journal of GEOMATE, Aug., 2018 Vol.15, Issue 48, pp.195-201
Geotec., Const. Mat. & Env., DOI: https://doi.org/10.21660/2018.48.74149
ISSN: 2186-2982 (Print), 2186-2990 (Online), Japan

STABILITY CHART FOR UNSUPPORTED SQUARE TUNNELS IN HOMOGENEOUS UNDRAINED CLAY

Jim Shiau[1], Mohammad Mirza Hassan[1] and Zakaria Hossain[2]

[1]School of Civil Engineering and Surveying, University of Southern Queensland, Australia
[2]Faculty of Bioresources, Mie University, Tsu, Japan

*Corresponding Author, Received: 14 March 2018, Revised: 13 April 2018, Accepted: 14 May 2018

ABSTRACT: This short technical note investigates the stability of a plane strain square tunnel in homogeneous undrained clay using shear strength reduction technique. The finite difference program *FLAC* is used to determine the factor of safety for unsupported square tunnels where an automatic generation of program script is developed using *FISH* programming. This developed procedure enables parametric studies to be conducted in an effective way with great efficiency. Numerical results, expressed in term of factor of safety, are compared with published classical upper and lower bound limit solutions. The comparison between these two numerical methods finds a very good agreement and the confidence level of the current *FLAC* model has increased significantly. With the success of model validations, a number of stability design charts for square tunnels using dimensionless ratios are presented for practical scenarios in a similar way to Taylor's slope stability charts. Examples are illustrated to show the potential usefulness of the produced design charts for practicing engineers.

Keywords: Square tunnel, Undrained clay, Stability, Strength reduction method, Design Chart

1. INTRODUCTION

Soil stability is one of the primary design criteria in any tunnel project. Correctly analysing the stability of underground infrastructure is crucial to prevent the collapse of the tunnel structure. This stability problem for undrained clay is best known by using the stability number (N) proposed by [1]. The stability number was initially defined in Eq. (1).

$$\boldsymbol{N} = \frac{\sigma_s + \gamma\left(C + \frac{D}{2}\right) - \sigma_t}{S_u} \tag{1}$$

Where σ_s is the uniform surcharge pressure on the surface and σ_t is the uniform internal tunnel pressure. The dimension of the square tunnel is ($W*D$) and the tunnel lies at a depth C below the ground surface. The undrained shear strength of soil and the unit weight of the soil are given by S_u and γ respectively. Note that this definition is not sustained for drained materials where volume changes during the shearing process and the shear strength is a function of the normal stresses.

The undrained stability number presented in Eq. (1) was re-defined and approached by the upper and lower bound solutions [2-5]. The problem was formulated as to find the limiting value of an overburden pressure ratio $(\sigma_s - \sigma_t)/S_u$ that is a function of the independent parameters such as the depth ratio C/D and the strength ratio $\gamma D/S_u$. Other similar tunnel stability research such as using pressure relaxation and finite difference methods can be found in [6 – 11]. It is possible to further simplify this stability number by neglecting σ_s and σ_t to simulate an unsupported excavation in green-field conditions. The problem is reduced to a simpler factor of safety problem, by assuming both of σ_s and σ_t equalling zero, which is a function of the depth ratio C/D and the strength ratio $S_u/\gamma D$ (or $\gamma D/S_u$). This approach is very similar to Taylor's design chart for slope stability analysis [12].

Following [5], this technical note investigates the stability of square tunnels in undrained clay. A strength reduction technique is used to determine the factor of safety of square tunnels in cohesive soils over a wide parametric range in green-field conditions. Results obtained from the strength reduction technique in *FLAC* [10] are compared to those published using the finite element limit analysis *FELA* [5]. A series of stability charts using the *FoS* approach is produced for practical applications.

2. PROBLEM STATEMENT

Tunnelling is a complex three dimensional problem in nature and therefore it is often reduced to a two dimensional one by assuming the transverse section as a very long tunnel. Figure 1 shows the problem statement for a 2D idealised model.

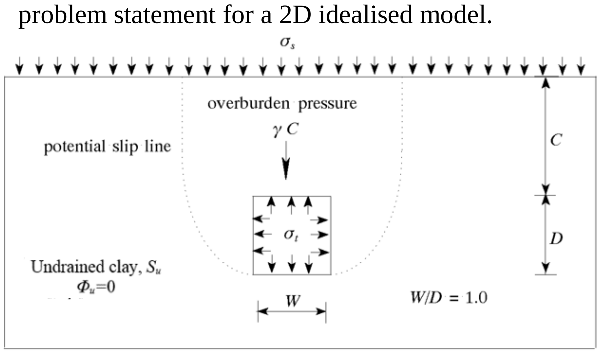

Fig. 1 Statement of problem (W/D = 1.0)

The soil body is considered as undrained and modelled as a uniform Tresca material with the undrained shear strength (S_u) and the saturated unit weight (γ), which is the same as a Mohr-Coulomb material when the soil frictional angle is zero. The dimension of the square tunnel is ($W*D$) and the cover depth is C. The soil strength ratio (*SR*) is represented by $S_u/\gamma D$. The factor of safety (*FoS)* is used to represent the stability of the square tunnel that is a function of the depth ratio (*C/D)* and strength ratio ($S_u/\gamma D$).

$$FoS = f\left(\frac{C}{D}, \frac{S_u}{\gamma D}\right) \tag{2}$$

To cover most realistic cases and to ensure that the *FoS* design charts produced can be applied to many different tunnel design, the parameters used in this study are $S_u/\gamma D$ = 0.2 - 2 and *C/D* = 1 - 6. The effects of surcharge σ_s and internal support pressure σ_t are not studied in this paper.

3. *FLAC* MODEL AND SHEAR STRENGTH REDUCTION METHOD (SSRM)

Over the last two decades, numerical modelling has proceeded to become a dominant technique for geotechnical stability problems. The shear strength reduction method is commonly used for slope stability analysis using finite element or finite difference methods. But in tunnel stability analysis, this method remains uncommon. With the advent of powerful computers and simulation programs in recent years, the shear strength reduction method is gradually being considered as an alternative method for tunnel stability analysis.

In the shear strength reduction method (*SSRM*), the shear strength of the material is reduced until the limiting condition is found where a factor of safety can be defined. The factor of safety is defined as a ratio of the strength necessary to maintain limiting equilibrium with the soil's available strength. If failure occurs initially, then the cohesion and friction angle is increased until limiting equilibrium or failure state is reached. Once the actual and critical strength are known, it is possible to calculate the factor of safety.

The factor of safety (*FoS*) being studied in this note are computed through finite difference code *FLAC*. Although the code is based on the explicit finite difference method, it is not very different from a nonlinear finite element program. A *FISH* script was developed to generate the mesh in *FLAC* and solve for the solution automatically. Using the script, parametric studies can be conducted efficiently and effectively with a quick change of input parameters (geometry and material).

Figure 2 shows a typical finite difference mesh of the problem in this study. The soil domain size for each case was selected to be large enough so that the failure zone is placed well with the domain. Note that the base and sides of the model is restrained in the *x* and *y* directions. For those nodes along the symmetrical line, only the x translation is restrained. The boundary conditions are important, so as to ensure that the entire soil mass is modelled accurately despite using a finite mesh.

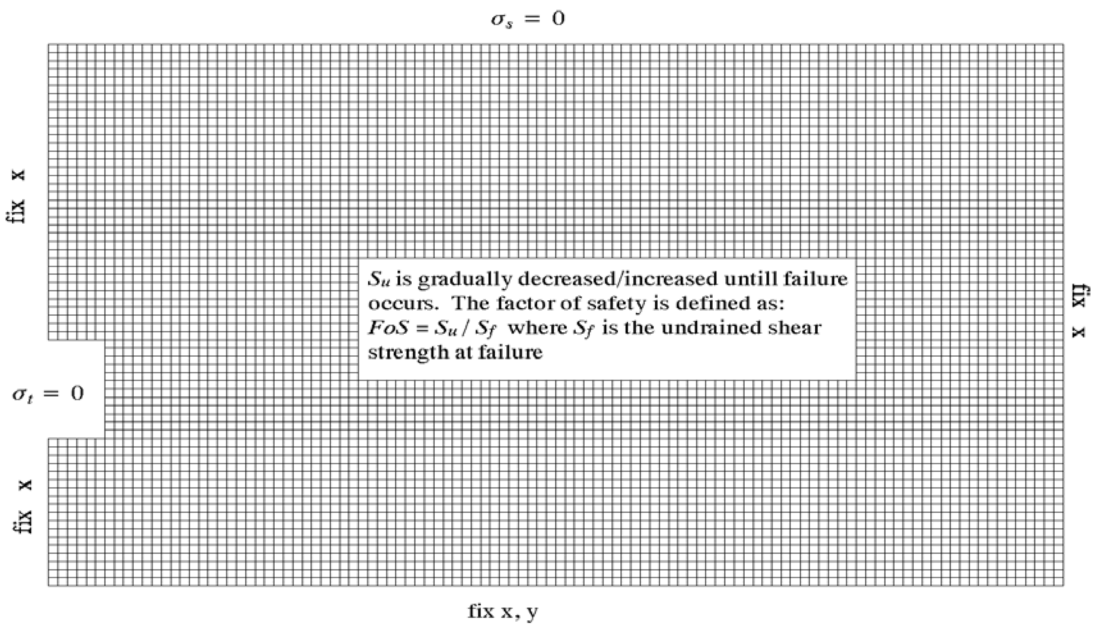

Fig. 2 Typical half mesh and boundary conditions (*W/D* = 1.0)

4. RESULTS AND DISCUSSION

Using the strength reduction technique in the finite difference program *FLAC*, factor of safety (*FoS*) values were obtained for a range of parameters in undrained clay. This parametric study covered dimensionless parameters, such as the depth ratio (*C/D*) and the strength ratio ($SR = S_u/\gamma D$). As stated above, the parameters used in this study are $S_u/\gamma D$ = 0.2 - 2 and *C/D* = 1 - 6.

Table 1 *FoS* results *(C/D=1, 2, and 3)*

C/D	$S_u/\gamma D$	*FLAC* (Finite Difference) *SSRM**
1	0.2	0.35
	0.4	0.71
	0.6	1.06
	0.8	1.42
	1.0	1.77
	1.3	2.30
	1.6	2.83
	2	3.54
2	0.2	0.27
	0.4	0.54
	0.6	0.81
	0.8	1.08
	1.0	1.35
	1.3	1.76
	1.6	2.16
	2	2.70
3	0.2	0.22
	0.4	0.45
	0.6	0.67
	0.8	0.90
	1.0	1.13
	1.3	1.46
	1.6	1.80
	2	2.25

** Shear Strength Reduction Method (SSRM)*

Table 1 presents the numerical results obtained in this study. Graphical comparisons are also presented in fig.3 - 5. In fig.3, *FoS* increases linearly as the strength ratio $S_u/\gamma D$ increases, indicating that there exists a stability number where the effective *FoS* is equal to one, a critical strength ratio $(SR)_c$. This could be achieved by dividing the strength ratio ($SR = S_u/\gamma D$) by the *FoS* result for each case i.e. the critical strength ratio $(SR)_c = S_u / (\gamma D FoS)$. Alternatively a *FoS* = 1 horizontal line can be drawn in Fig. 3 and the corresponding ($S_u/\gamma D$) values are the critical $(SR)_c$. Note that the rate of *FoS* increase is different for each *C/D* value. The gradient of the line is greater for smaller *C/D* values.

Table 2 *FoS* results *(C/D=4, 5, and 6)*

C/D	$S_u/\gamma D$	*FLAC* (Finite Difference) *SSRM**
4	0.2	0.20
	0.4	0.39
	0.6	0.59
	0.8	0.78
	1.0	0.98
	1.3	1.27
	1.6	1.56
	2	1.96
5	0.2	0.18
	0.4	0.35
	0.6	0.53
	0.8	0.71
	1.0	0.88
	1.3	1.15
	1.6	1.41
	2	1.76
6	0.2	0.16
	0.4	0.32
	0.6	0.47
	0.8	0.63
	1.0	0.79
	1.3	1.03
	1.6	1.27
	2	1.59

** Shear Strength Reduction Method (SSRM)*

Figure 4 shows that the *FoS* decreases nonlinearly with increasing depth ratio *C/D* for all strength ratios defined as $S_u/\gamma D$. It should be noted that the strength ratio is normalised with respect to the γD, and the undrained shear strength (S_u) remains constant throughout the increasing depth ratios. When *C/D* increases and the undrained shear strength (S_u) remains constant, the results of *FoS* values decreases due to the increasing overburden pressure (γC). This is in contrast to the common belief that an increase to *C/D* always results in an increase to *FoS* where arching effect plays an important role in this phenomenon.

A simple observation can be made from Fig.1, where the active force is the weight of soil and the resisting force is given by the shear strength of the soil. Of two hypothetical tunnels in the same cohesive soil but at different depths, the tunnel with the smaller active force (γC) will have a higher probability of stability. This observation may not be true in a soil with internal friction angle due to the additional shear strength from the second term of the shear strength equation ($\sigma \tan\phi$) and the geometrical arching effects. In purely cohesive soils, the latter still occurs, but its effect is not enough to overcome that subsequent increase in active force.

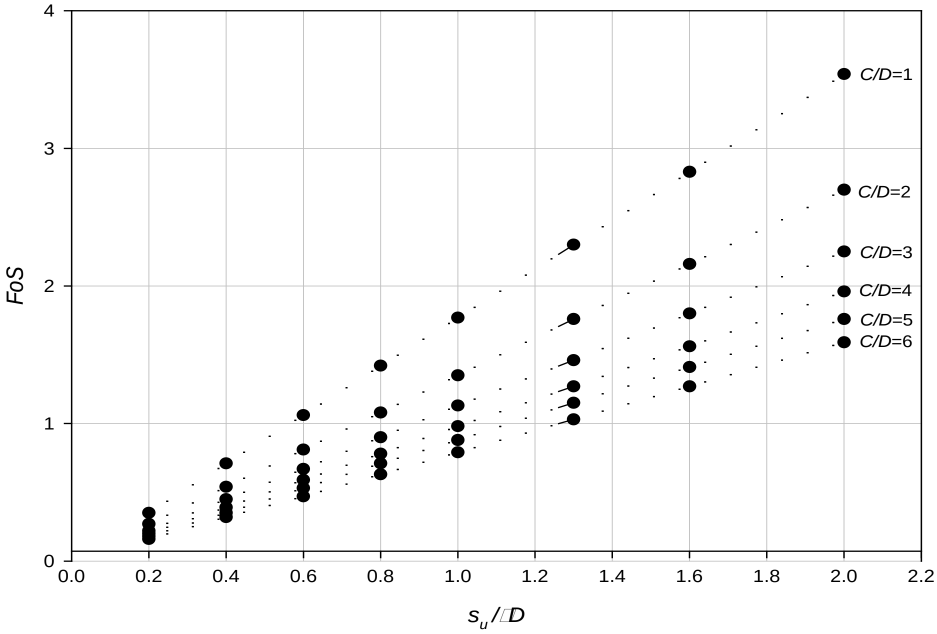

Fig. 3 Comparison of *FoS* results with respect to $S_u/\gamma D$ for various values of *C/D*

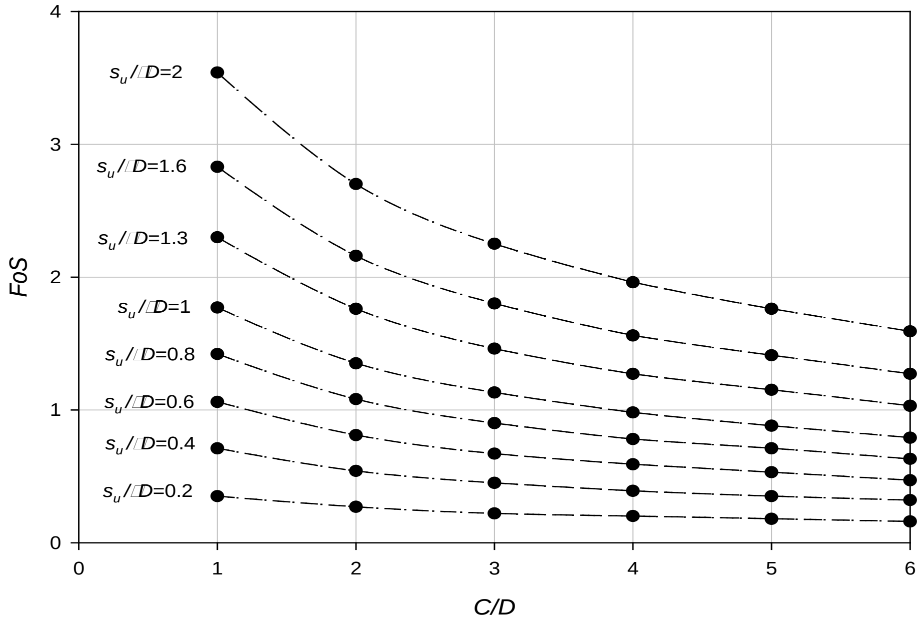

Fig. 4 Comparison of *FoS* results with respect to *C/D* for various values of $S_u/\gamma D$

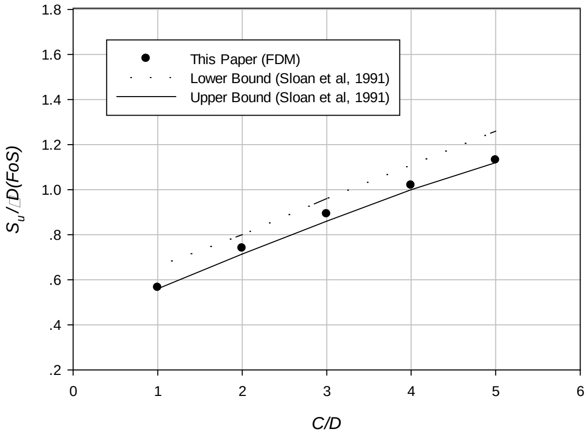

Fig. 5 Comparison of critical strength ratio $(SR)_c = S_u/\gamma D(FoS)$

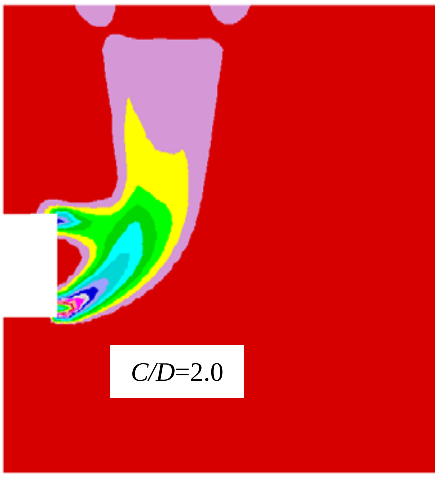

Fig. 6 Plot of shear strain rate for C/D=2.0 and $S_u/\gamma D$ = 0.4

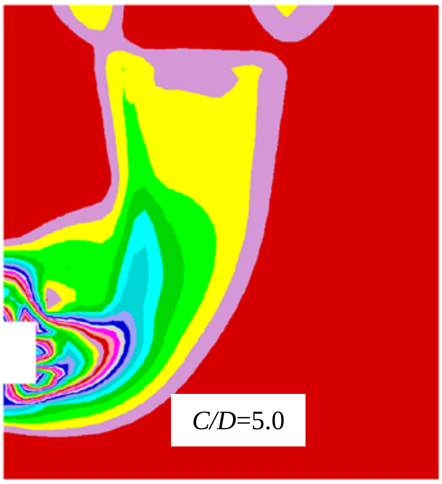

Fig. 7 Plot of shear strain rate for C/D=5.0 and $S_u/\gamma D$ = 0.4

It is important to compare the finite difference estimates with the rigorous finite element upper and lower bounds based on the limit theorems of classical plasticity [5]. This comparison is shown in fig.5 . The critical strength ratio $(SR)_c = S_u / (\gamma DFoS)$ is presented with various depth ratios *(C/D)*. Note that the finite difference results produced in this paper are in good agreement with the upper and lower bound solutions.

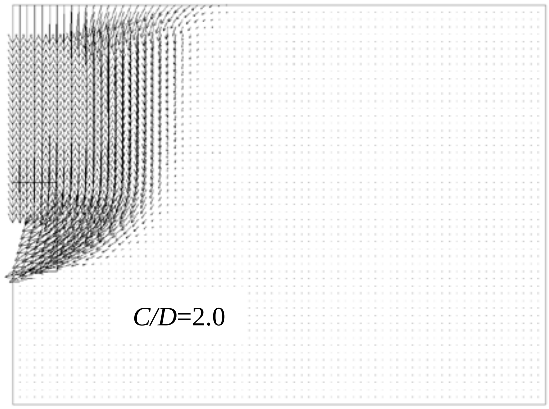

Fig. 8 Velocity field for C/D=2.0 and $S_u/\gamma D$ = 0.4

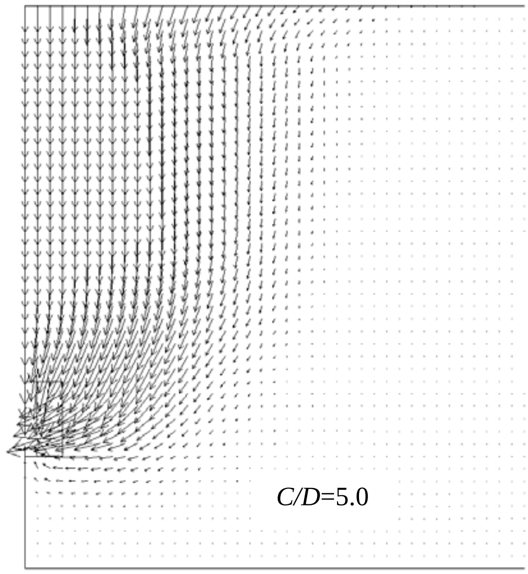

Fig. 9 Velocity field for C/D=5.0 and $S_u/\gamma D$ = 0.4

Figures 6-9 show some typical plots of the shear strain rate and velocity field from the program output. This information of failure extent is important as it will assist practising engineers in making a decision in relation to the monitoring of ground movements. It was noted in this study that the strength ratios, $SR = S_u/\gamma D$, have no direct impact on the failure extent. This can be understood from the computational nature of the shear strength reduction method. However, the information of the extent of failure surface for various depth ratios *C/D* is useful for practical engineers. The actual values of these non-zero shear strain rates are not important and therefore they are not show in the plot. They are not real strains for the perfectly plasticity soil model. The plot simply indicates the potential failure surface.

Figures 10 and 11 show typical principal stress tensor plots. They are normally used to demonstrate the potential effects of arching phenomenon. These plots show the directions of major and minor principal stresses, indicating weak soil arching throughout the soil body. As discussed, soils with an internal friction angle ($\phi \neq 0$) would have more potential for stability, with the internal frictional angle adding to the strength of the material by the soil arch.

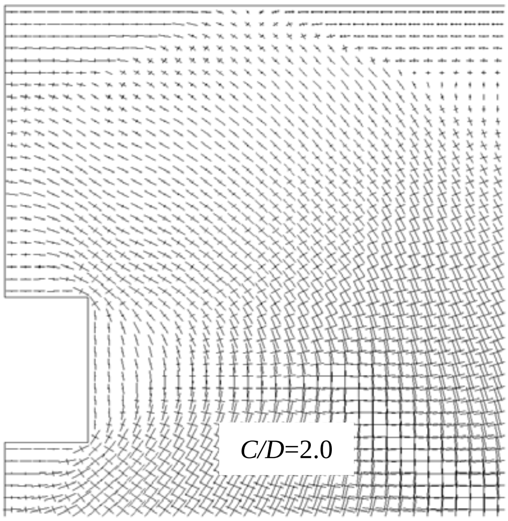

Fig. 10 Principle stress tensor plot at collapse for C/D=2.0 and $S_u/\gamma D$ = 0.4

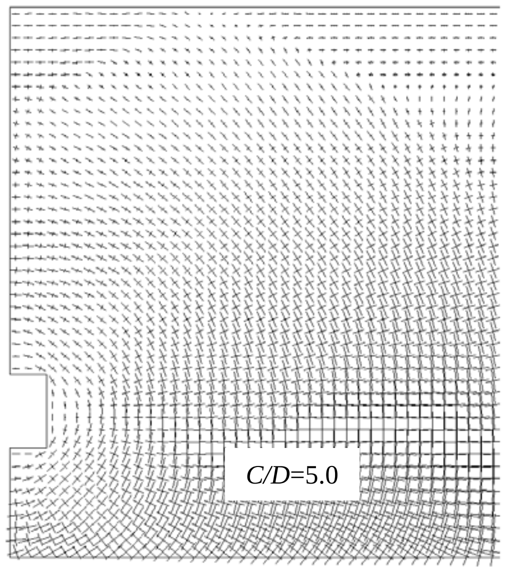

Fig. 11 Principle stress tensor plot at collapse for C/D=5.0 and $S_u/\gamma D$ = 0.4

5. THE STABILITY CHART

The stability design chart is best demonstrated through a number of examples. Using the numerical results presented in Table 1, a contour design chart for *FoS* has been produced in fig.12 that can be used by tunnel engineers to relate the depth ratio (C/D), soil strength ratio ($S_u/\gamma D$) and factor of safety (*FoS*). Regression of the design chart gives the following relationship (Eq.3) with r^2 = 0.996

$$\boldsymbol{FoS = 1.8\left(\frac{S_u}{\gamma D}\right)\left(\frac{C}{D}\right)^{-0.45}} \qquad (3)$$

Using the design chart (fig.12) and Eq. (3), the following practical examples are illustrated for either analysis or design purposes.

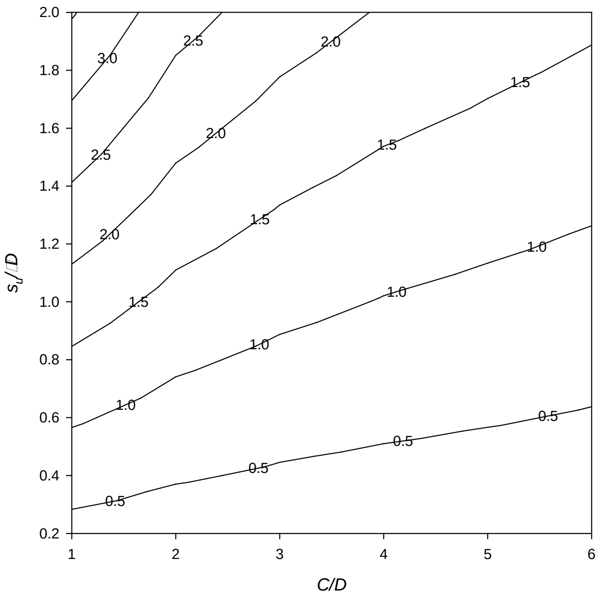

Fig. 12 Stability chart for *FoS* with respect to *C/D* and $S_u/\gamma D$

5.1 Analysis of an Existing Square Tunnel

For an existing unsupported square tunnel without surcharge load **(**σ_s**)** and capacity to provide internal supporting pressure **(**σ_t**)**, determine the factor of safety of the tunnel given the parameters S_u = 50 kPa, γ = 18 kN/m^3, C = 18 m, and $D = W =$ 6 m.

1. Using C/D = 3.0, $S_u/\gamma D$ = 0.46, Eq.3 gives a *FoS* of 0.51.
2. Using C/D = 3.0, $S_u/\gamma D$ = 0.46, Fig.12 gives an approximate *FoS* of 0.53.

An actual computer analysis of this particular case gives a *FoS* of 0.52.

5.2 Design of an Unsupported Square Tunnel

The soil properties are known at the tunnel project site, and the dimension is specified. A target factor of safety is chosen, and the designers need to specify a maximum cover depth that will satisfy the target *FoS*. Parameters are given as: S_u = 135 kPa, γ = 18 kN/m^3, D = W = 6 m, and the target *FoS* = 1.5.

1. Using *FoS* = 1.5 and $S_u/\gamma D$ = 1.25, Eq.3 gives a C value of 14.77 m (C/D = 2.46).
2. Using *FoS* =1.5 and $S_u/\gamma D$ = 1.25, Fig.12 gives an approximate C/D value of 2.60 and therefore C value of 15.60 m.

An actual computer analysis for this particular case (C value of 15.0m) gives a *FoS* of 1.53.

6. CONCLUSION

Stability of plane strain square tunnels has been investigated in this technical note using shear strength reduction method provided within *FLAC*. The comparison between rigorous upper and lower bound limit solutions and the shear strength reduction solutions found a very good agreement. Design charts and equation were produced and examples illustrated on how to use them. The factor of safety approach to tunnel stability problems, similar to Taylor's chart for slope stability analysis and design, does provide useful information for practical engineers at their preliminary design stage. The current research shall be extended to cover the effects of soil friction angle (ϕ), surcharge (σ_s) and internal pressure (σ_t) in the future.

7. REFERENCES

[1] Broms, BB & Bennermark, H 1967, Stability of clay at vertical openings, Journal of the Soil Mechanic and Foundations Division, Proceedings of the American Society of Civil Engineers, vol. 93, pp. 71- 93.

[2] Davis, EH, Gunn, MJ, Mair, RJ & Seneviratne, HN 1980, The stability of shallow tunnels and underground openings in cohesive material, Geotechnique, vol. 30, pp. 397-416.

[3] Sloan, SW 1988, Lower bound limit analysis using finite elements and linear programming, International Journal for Numerical and Analytical Methods in Geomechanics, vol. 12, pp. 61-67.

[4] Sloan, SW 1989, Upper bound limit analysis using finite elements and linear programming, International Journal for Numerical and Analytical Methods in Geomechanics, vol. 13, pp. 263-282.

[5] Sloan, SW and Assadi, A 1991, Undrained stability of a square tunnel in a soil whose strength increases linearly with depth, Computers and Geotechnics, 12, pp. 321-346.

[6] Shiau, J, Sams, M and Chen, J 2016, Stability charts for a tall tunnel in undrained clay, Int. J. of GEOMATE, vol. 10(2), pp. 1764-1769

[7] Shiau, J, Sams, M and Lamb, B 2016, Introducing advanced topics in geotechnical engineering teaching – Tunnel Modelling, Int. J. of GEOMATE, vol. 10(1), pp. 1698-1705

[8] Shiau, J, Lamb, B and Sams, M 2016, The use of sinkhole models in advanced geotechnical engineering teaching, Int. J. of GEOMATE, vol. 10(2), pp. 1718-1724

[9] Shiau, J and Sams, M 2017,Estimation of tunneling induced ground settlement using pressure relaxation method, Int. J. of GEOMATE, vol. 13(39), pp. 132-139

[10] Shiau, J, Sams, M, Lamb, B, and Lobwein, J 2017, Stability charts for unsupported circular tunnels in cohesive soils, Int. J. of GEOMATE, vol. 13(39), pp. 95-102

[11] Shiau, J, Sams, M, Al-Asadi, F and Hassan, MM, Stability charts for unsupported plane strain tunnel headings in homogeneous undrained clay, Int. J. of GEOMATE, vol. 14(41), pp. 19-26

[12] Taylor, DW 1937, Stability of earth slopes. Journal of the Boston Society of Civil Engineers, vol. 24, no. 3, pp. 197-246.